# PIN and CCCH Zn-Finger domain coordinate RNA targeting in ZC3H12 family endoribonucleases

**Ankur Garg[1,2,4 #], Yvette Roske[1], Shinnosuke Yamada[3], Takuya Uehata[3], Osamu Takeuchi[3] and Udo Heinemann[1,2 #]**

[1] Macromolecular Structure and Interaction, Max-Delbrück Center for Molecular Medicine in the Helmholtz Association, Robert-Rössle-Str. 10, 13125 Berlin, Germany

[2] Institute for Chemistry and Biochemistry, Freie Universität Berlin, Takustr. 6, 14195 Berlin, Germany

[3] Department of Medical Chemistry, Graduate School of Medicine, Kyoto University, Kyoto, Japan

[4] Current address: W.M. Keck Structural Biology Laboratory, Cold Spring Harbor Laboratory, 1 Bungtown Road, Cold Spring Harbor, New York 11724, USA

[#] To whom correspondence should be addressed

## Supplementary Material

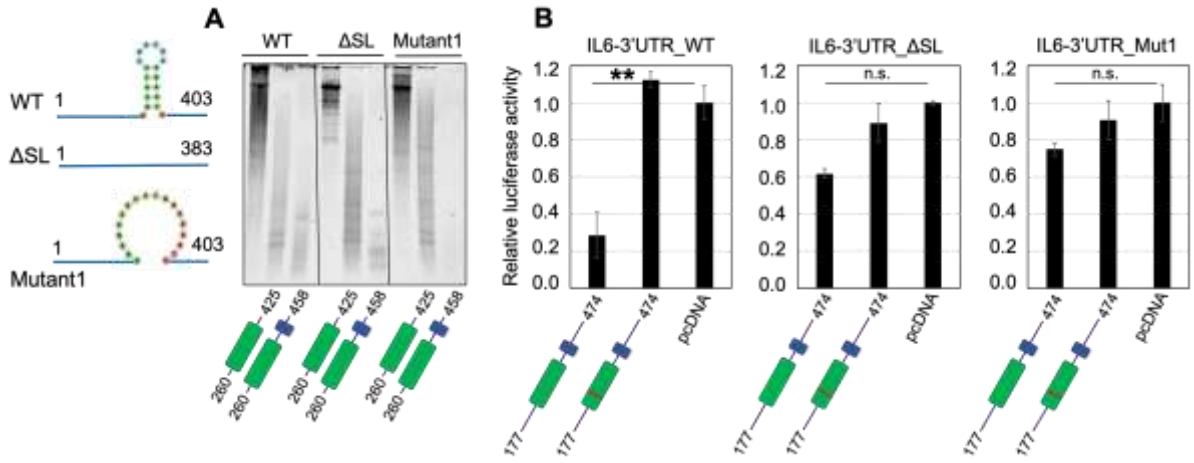


**Figure S1**. (A) 6% urea-PAGE demonstrating non-specific *in vitro* degradation of IL-6 3'UTR RNA variants by ZC3H12C. The ZC3H12C PIN$^{260-425}$ and PIN-Zf$^{260-458}$ constructs degrade different RNA substrates (WT, ΔSL and mutant1) implicating involvement of an adaptor protein in regulating *in vivo* RNase activity. Designed RNA substrates are depicted on the left, and marked on top of the wells in gel. (B) Luciferase reporter assay showing *in vivo* RNase activity of ZC3H12C N-PIN-Zf-C$^{177-474}$. The additional N- and C-motifs likely present regulatory elements leading to a regulated response against the IL-6 3'UTR, a well know target for ZC3H12A. The D271N catalytic mutant (marked with a red bar in the PIN domain) exhibits no activity *in vivo*. The domain architecture of the used protein constructs is shown at the gel and graph bottom with PIN domain in green and the ZFD shown in blue. Data are presented as mean ± SD (n=3). **, P < 0.01 (two-tailed Student's *t*-test). n.s., not significant.

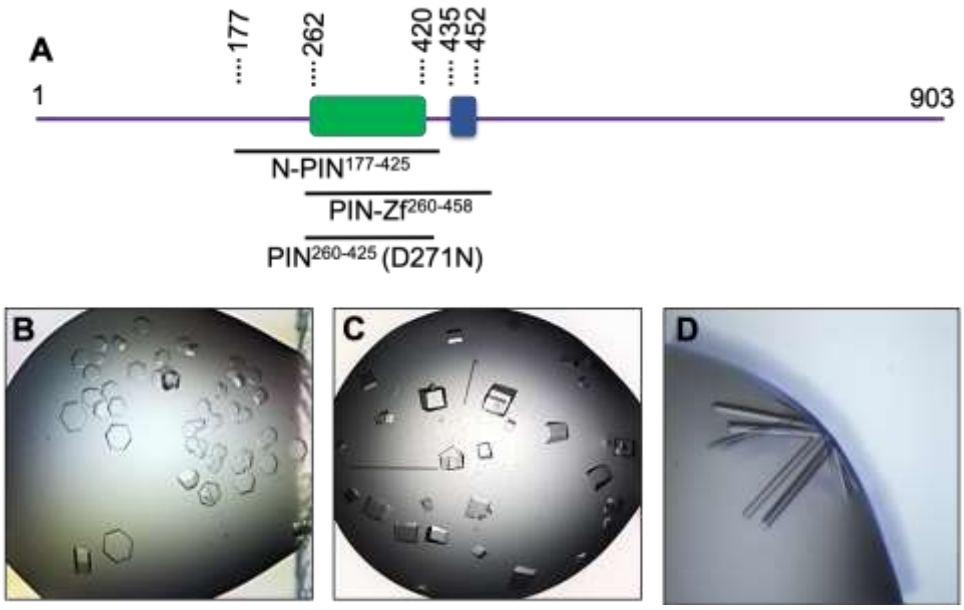


**Figure S2**. Crystallization of ZC3H12C protein variants. (A) Domain architecture of *Mm*ZC3H12C showing the PIN/RNase domain (green) and the CCCH-type ZFD (blue) conserved in all members of the Regnase/ZC3H12 family. Underlined, details of crystallized constructs with their amino-acid boundaries given as superscripts. (B) Crystalline hexagons of N-PIN$^{177-425}$ were obtained using 0.2 M LiCl, 50 mM $MgSO_4$ and 8% PEG 8000 as reservoir buffer. (C) PIN-Zf$^{260-458}$ crystals grew as cubes in 0.2 M LiCl, 20% PEG 6000 and 0.1 M HEPES pH 7.0 as reservoir solution. (D) Crystalline rods of PIN$^{260-425}$(D271N) grew in 0.2 M KSCN, 20% PEG 3350 and 0.1 M Bis-Tris propane pH 6.5 as reservoir solution.

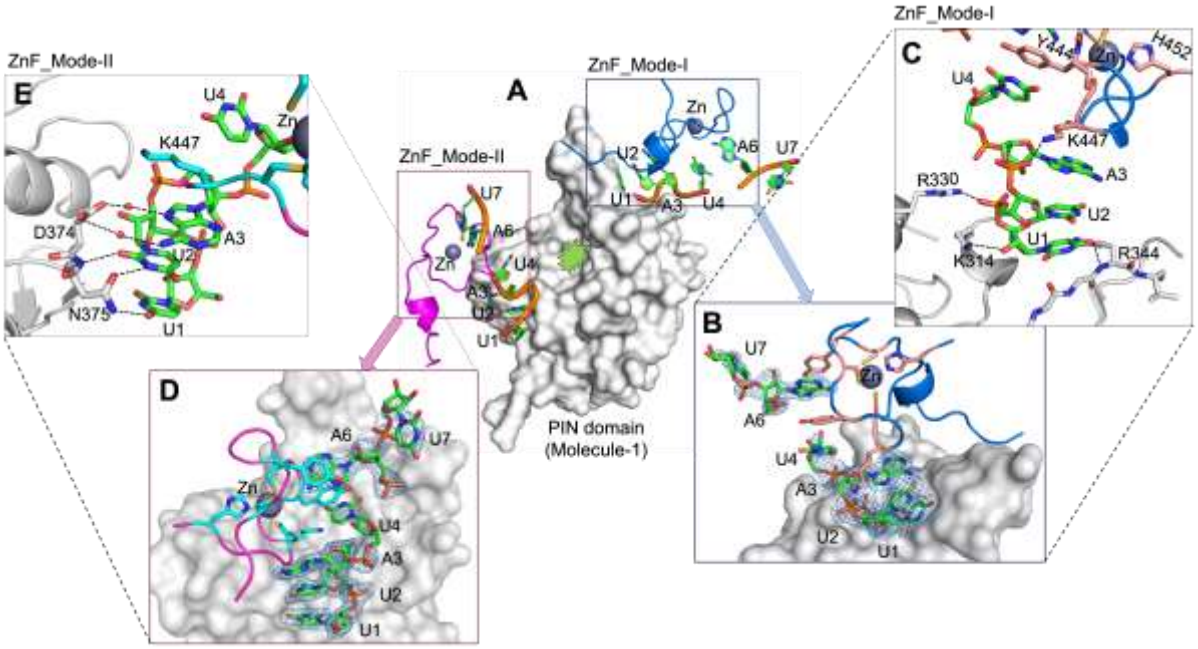


**Figure S3**. Two modes of ZFD-bound RNA docking onto the ZC3H12C PIN domain. (A) Surface representation of the *Mm*ZC3H12C_PIN domain (gray) with two CCCH Znf-RNA complexes from neighboring protein molecules, docked in different orientations (ZnF mode-I and ZnF mode-II). The two ZnF-RNA complexes are shown as cartoon, with ZnFs colored blue in mode-I and magenta in mode-II. (B) The rU1 nucleotide is docked onto the positively charged surface on the PIN domain in mode-I and rA3 is stacked under the Lys447 side chain. (C) Molecular interactions between PIN domain and RNA in mode-I with multiple hydrogen bonds involving positively charged residues (K314, R330 and R344) and ribo-nucleotides depicted by dotted lines. (D) In mode-II, the ZnF-RNA complex is docked near the catalytic site (green asterisk) of the RNase domain. (E) The RNA is bound by multiple hydrogen bonds between N375 and D374 and the Watson-Crick edges of rU1, rU2 and rA3. The ZnF additionally stabilizes the RNA by U4 and A6 base stacking in both mode-I and mode-II. The RNA strand is shown as sticks with $2DF_o$-$mF_c$ electron density contoured at 0.9 σ with 1.6 Å radius of atoms. The electron density for the rU1, rU2, rA3 and rA6 nucleotides is strong, while the rU4 and rU7 nucleotides exhibit slightly weaker electron density. The rU5 is cleaved and shows no electron density in the structure.

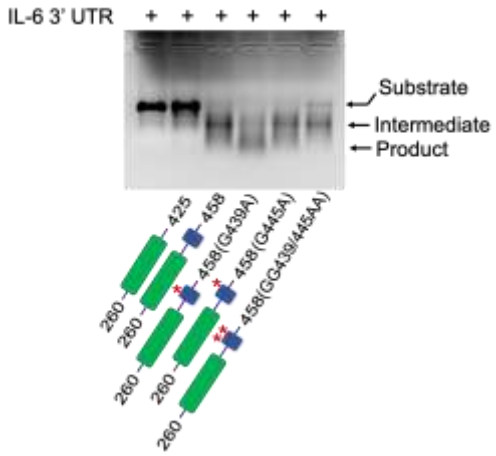


**Figure S4**. RNA hydrolysis by the unique ZC3H12C ZnF glycine mutants after just 5 min incubation with IL6-3'UTR analyzed on a 1.2% denaturing agarose gel. The G439A mutant shows higher activity than WT (PIN-Zf$^{260-458}$) and produces significantly more product RNA, implicating that G439 induced backbone bending in the ZnF is crucial in controlled RNase activity. The PIN domain is shown in green and the ZFD in blue, with glycine mutations also shown in the domain diagrams (bottom).